Site-Ordered Solids

DOI: 10.1002/ange.200500135

$Ba_8CoNb_6O_{24}$: A d^0 Dielectric Oxide Host Containing Ordered d^7 Cation Layers 1.88 nm Apart**

*Phillip M. Mallinson, Mathieu M. B. Allix, John B. Claridge, Richard M. Ibberson, David M. Iddles, Tim Price, and Matthew J. Rosseinsky**

The search for multiproperty materials,[1] in which one cooperative phenomenon can control another through modulation of the local structure and bonding, is complicated by the need to separate the chemical units responsible for these different properties. Thus, rules are required for the synthesis of materials that assemble with spatial segregation of the elements conferring distinct properties. These rules should be sufficiently strict to operate at the high synthesis temperatures required for processing many inorganic materials.

This challenging synthetic task can be addressed by exploiting the diversity of site chemistries[2] available in a complex perovskite structure and harnessing the combination of the specific bonding requirements of the d^0 cations and the site symmetries in the structure to drive the cation ordering. Here we present the functional material $Ba_8CoNb_6O_{24}$ comprising isolated single layers of Co^{2+} d^7 cations separated by intervening d^0 cation layers and 1.88 nm away from the next Co^{2+} layer. Most remarkable is that this long-range ordering is driven despite the low concentration of Co^{2+} cations in the structure. These site-ordered solids are then processed to permit their evaluation as microwave dielectric resonators.

In the chemistry of transition-metal oxides, elements in the d^0 oxidation state (particularly Ta^V, Ti^{IV}, and Nb^V), with their characteristic directional M–O multiple bonding, are the basic components of ferroelectric, relaxor, and high-permittivity materials.[3] Transition-metal centers that bear d electrons (d^n centers) confer magnetic, optical, and electronic properties on materials. The development of extended metal oxide networks in which d^n centers can be separated by long distances with precise site order within a d^0 matrix offers great potential in materials design. The ordering of cations of different sizes and charges is possible on the octahedral B site of the ABO_3 perovskite structure[4]—hexagonal stacking of the AO_3 close-packed layers produces face-sharing octahedral sites in addition to the corner-sharing sites characteristic of a cubic stacking sequence. The face-sharing sites thus introduced are favorable locations for cation vacancies, with mixed hexagonal and cubic stacking sequences resulting in the family of "hexagonal perovskites".[5]

Complex tantalum oxides are widely employed as microwave resonators in mobile telecommunications, but the cost of raw materials makes niobium-based alternatives desirable. The eight-layer hexagonal perovskite $Ba_8ZnTa_6O_{24}$ adopts a $(chcc)_2$ sequence (an AO_3 layer (B) is described as h if its two neighboring layers are the same (ABA) or c if they are different (ABC)) and has interesting dielectric properties with a moderately high Q of 20800 at 3.28 GHz ($Q = (\tan\delta)^{-1}$).[6] Our initial investigations on the Nb analogue $Ba_8ZnNb_6O_{24}$ consistently lead to the synthesis of polyphasic material with several competing stacking sequences of hexagonal and cubic layers.

Investigation of the cobalt-substituted niobate $Ba_8CoNb_6O_{24}$ revealed that this composition afforded single-phase material with an eight-layer ($c \approx 18$ Å , BaO_3 layer thickness ≈ 2.3 Å) repeat in contrast to the mixed phases in the Ba-Zn-Nb-O field at this composition. Surprisingly, although $Ba_8CoTa_6O_{24}$ is isostructural with $Ba_8ZnTa_6O_{24}$ and tolerance factor effects associated with stacking sequence changes[5] are absent, the new Nb phase adopts a different eight-layer stacking sequence in which two hexagonal ABA AO_3 layer units are adjacent to each other in an ccchhccc motif (Figure 1).[7] High-resolution electron microscopy images directly demonstrate that this sequence is adopted without stacking faults (Figure 2a). The $P\bar{3}m1$ space-group symmetry is confirmed by electron diffraction (Figure 2b,c) and the cation composition and homogeneity by energy dispersive spectroscopy (EDS) in the electron microscope. Although all the occupied octahedra in such a sequence are corner sharing, and the triple layer of face-sharing octahedral sites in the hh region of the structure

[*] P. M. Mallinson, Dr. M. M. B. Allix, Dr. J. B. Claridge, Prof. M. J. Rosseinsky
Department of Chemistry
The University of Liverpool
Liverpool L69 7ZD (UK)
Fax: (+44) 151-794-3587
E-mail: m.j.rosseinsky@liverpool.ac.uk
Dr. R. M. Ibberson
ISIS Facility
CCLRC – Rutherford Appleton Laboratory
Chilton, Didcot
Oxon OX11 0QX (UK)
Dr. D. M. Iddles, T. Price
Filtronic Comtek, Ceramics Division
Enterprise Drive, Station Road, Four Ashes
Wolverhampton WV10 7DB (UK)

[**] We thank EPSRC for Portfolio Partnership funding and CCLRC and the CCLRC Centre for Materials Physics and Chemistry for partial support of P.M. (grant ref. CMPC03106).

Supporting information for this article is available on the WWW under http://www.angewandte.org or from the author.

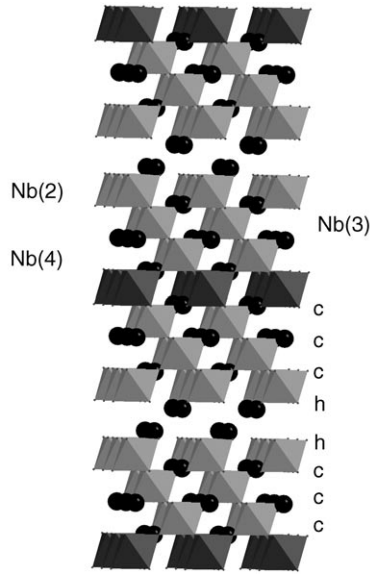

Figure 1. The cchhccc stacking sequence of $Ba_8CoNb_6O_{24}$ shows strict ordering of the Co^{2+} cations (comprising only 12.5% of the total octahedral-site cations) on the central layer of octahedral sites within the seven-block unit of corner-sharing octahedra. Cobalt- and niobium-centered octahedra are shown in dark gray and light gray, respectively, and barium cations are represented as black spheres. The layer of vacant octahedral sites in the hh region of the stacking sequence produces a structure consisting solely of corner-sharing octahedra.

results in a central layer of vacant sites (Figure 1), $Ba_8CoNb_6O_{24}$ displays essentially complete ordering of the Co^{2+} and Nb^{5+} cations. Refinement of high-resolution time-of-flight neutron powder diffraction data reveal the superiority of fully ordered ($\chi^2 = 2.92$) over fully disordered ($\chi^2 = 3.15$) models; permitting antisite disorder between the single Co (*1a*) and three crystallographically distinct Nb sites results in 95(3)% Co occupancy of the *1a* site and pure Nb(2) and Nb(3) sites within 1σ; improvements in agreement indices when site disorder was permitted were insignificant. (The atomic displacement parameters in the partially ordered model are unphysical, with several atoms refining to negative values, and the convergence was not robust). The fully site-ordered model was thus adopted (Table 1 and Table 2) The bond valence sums for Co^{2+} and Nb^{5+} on the *1a* site are 1.95 (3% deviation from expected) and 3.51 (30% deviation), respectively, while the maximum deviation from the ideal bond valence of 5 for Nb^{5+} cations on the other three sites in the structure is 8%. As the Nb^{5+} bond valence in fully site-ordered $Ba_3MgNb_2O_9$ is 4.66,[8] both the site occupancies and bond-valence considerations indicate that the cation site order is complete in $Ba_8CoNb_6O_{24}$.

The *1a* sites solely occupied by Co^{2+} are at the centers of the seven-layer blocks of corner-sharing octahedra. This is surprising as a statistical distribution of cobalt cations over the four available sites might have been expected given their low concentration (only 12.5% of the octahedral sites are occupied by Co^{2+}) and the existence of only corner-sharing sites in the structure. The *1a* site is the most regular environment amongst the four symmetry-inequivalent octahedral sites, as it is located necessarily at a center of symmetry

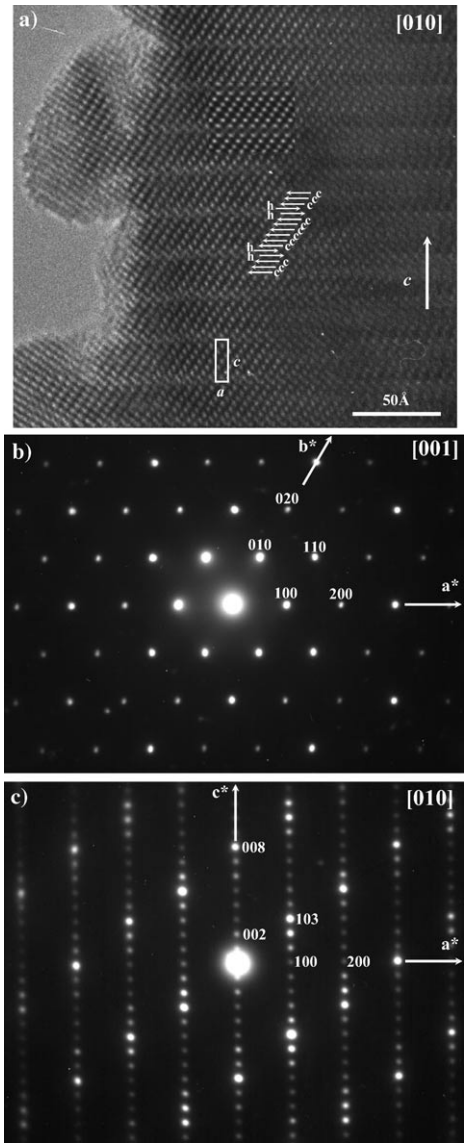

Figure 2. a) HREM image of $Ba_8CoNb_6O_{24}$ recorded along the [010] direction. The simulated image is embedded. Experimental [001] (b) and [010] (c) electron diffraction patterns.

as a result of the odd number of occupied layers in the stacking sequence. The symmetry-imposed requirement that all the bond lengths between oxygen and the central atom on this site are equal is inconsistent with the multiple-bonding preference of Nb^{5+}, which is often displaced from the center of an octahedral environment to form multiple bonds to oxygen (Figure 3a). This in turn favors all the Co^{2+} cations, which are more commonly found in centrosymmetric oxide octahedra (Figure 3b), occupying the site to avoid forcing Nb^{5+} into an unfavorable environment. The availability of the distinctly bonded *1a* site together with the cation charge difference (which is more pronounced here than between the cations with charges of +3, +4, and +5 of site-disordered $Ba_8In_{0.5}Ti_2Nb_{4.5}O_{24}$)[7] drives the strict site ordering and resulting extreme long-range separation of the cobalt cation layers. This strict site ordering results in the separation of Co^{2+} layers by 1.88 nm along *c*. Ordering over this distance

Table 1: Refined coordinates of $Ba_8CoNb_6O_{24}$. Space group $P\bar{3}m1$; $a = 5.789813(10)$, $c = 18.89355(6)$ Å; $\chi^2 = 2.9$ $R(F^2) = 5.88\,\%$ $R(F) = 4.34\,\%$. The global instability index,[14] which measures the mean deviation of the bond valence sum of all ions in the structure from their formal valence, is 0.21, which is consistent with that observed in high-permittivity niobates based on site-ordered cubic perovskites.[8] The weighted average deviation from the ideal bond valence sums is 0.058, which is consistent with those observed in cubic perovskite niobates. The valence sums at Ba of over 2 indicate compression around these sites, as is commonly observed in perovskite niobates.[8]

	x	*y*	*z*	100 U [Å^{-2}]	Symm.	Site	BVS[a]
Ba1	0	0	0.1862(2)	0.9(1)	3*m*	2c	2.45
Ba2	1/3	2/3	0.0609(3)	0.77(9)	3*m*	2d	2.32
Ba3	1/3	2/3	0.4564(2)	0.70(9)	3*m*	2d	2.08
Ba4	1/3	2/3	0.6826(2)	0.12(8)	3*m*	2d	2.51
Co1	0	0	0	0.1(2)	$\bar{3}m$	1a	1.95
Nb2	0	0	0.3849(1)	0.44(6)	3*m*	2c	4.93
Nb3	1/3	2/3	0.2549(2)	0.52(8)	3*m*	2d	4.64
Nb4	1/3	2/3	0.8789(1)	0.61(9)	3*m*	2d	4.58
O1	0.1679(2)	0.8321(2)	0.3074(1)	0.82(6)	*m*	6i	2.03
O2	0.1630(2)	0.8369(2)	0.5706(1)	1.05(6)	*m*	6i	2.15
O3	0.1710(3)	0.8289(3)	0.9351(1)	0.72(4)	*m*	6i	2.03
O4	0.4985(2)	0.5014(2)	0.1868(1)	0.92(6)	*m*	6i	1.94

[a] BVS is the bond valence sum for the atom.

Table 2: Bond lengths [Å] and angles [°] in $Ba_8CoNb_6O_{24}$. The magnitude of the off-center distortion at the Nb sites, computed as $1/6 \sum_{n=1,6} ((d_n - \bar{d})/\bar{d})^2$, where $\bar{d}$ is the mean bond length at the site, is 0.0094 (Nb2), 0.0017 (Nb3), and 0.0014 (Nb4) compared with 0.0016 in fully site-ordered $Ba_3MgNb_2O_9$.[8]

Co1–O3	×6	2.108(3)	Nb3–O1	×3	1.933(4)
O3-Co1-O3	×6	89.6(1)	Nb3–O4	×3	2.097(3)
O3-Co1-O3	×6	90.4(1)	O1-Nb3-O1	×3	96.0(2)
O3-Co1-O3	×3	180.0(1)	O1-Nb3-O4	×3	173.1(2)
			O1-Nb3-O4	×6	88.60(7)
Nb2–O1	×3	2.231(3)	O4-Nb3-O4	×3	86.3(2)
Nb2–O2	×3	1.837(3)			
O1-Nb2-O1	×3	81.6(1)	Nb4–O3	×3	1.942(4)
O1-Nb2-O2	×3	166.2(2)	Nb4–O4	×3	2.095(3)
O1-Nb2-O2	×6	87.9(1)	O3-Nb4-O3	×3	93.0(2)
O2-Nb2-O2	×3	100.8(2)	O3-Nb4-O4	×3	176.7(2)
			O3-Nb4-O4	×6	89.2(1)
			O4-Nb4-O4	×3	88.4(1)

over purely six coordinate sites is unusual (Mn^{2+} and W^{6+} are ordered within a three-layer block in $Ba_2La_2MnW_2O_{10}$, where the concentration of the centrosymmetric cation is considerably higher than the present case[9]), although discrete Fe^{3+} tetrahedral layers are observed separated by mixed iron/titanium octahedral layers in complex barium iron titanium oxides.[10]

The Nb(2) site adjacent to the layer of vacant octahedral sites has the most pronounced off-center displacement of Nb^{5+} towards a triangular face of the octahedral oxide environment along the threefold axis due to the absence of other cations competing for bonding with the O2 oxide anions. The other two Nb sites, which share all their coordinating oxide anions with neighboring B site cations, have off-center displacements similar to those observed in fully site-ordered $Ba_3MgNb_2O_9$,[8] in accord with the proposed structural model for $Ba_8CoNb_6O_{24}$. It is interesting to note that the separation of the BaO_3 layers neighboring the vacant site is at 1.65 Å consistent with that of $Ba_5Nb_4O_{15}$ but distinctly shorter than found in the Q blocks of ferrites,[11] where the corresponding distance is 2.15 Å.

Magnetization data for $Ba_8CoNb_6O_{24}$ obeyed the Curie–Weiss law between 2 and 300 K with an effective moment of 4.06 μ_B per Co (the spin-only value is 3.87 μ_B) and −4.26(6) K antiferromagnetic Weiss constant) and no irreversibility between field and zero-field cooled runs (Figure 4). This is consistent with the structural model of Co^{2+} cations with near-neighbor Co–Co distances within the layer of 5.786 Å without direct Co-O-Co superexchange pathways. Deviations from the spin-only prediction are commonly observed for

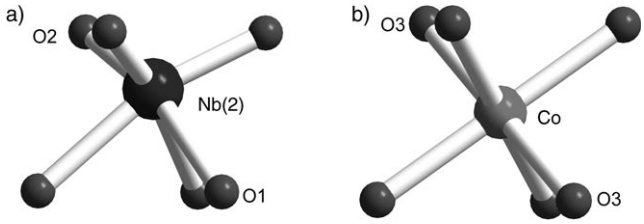

Figure 3. a) The asymmetric multiple bonding to oxide by Nb^{5+} produces displacement of Nb(2) from the center of the octahedron towards the face of three O2 oxide anions bordering the layer of vacant face-sharing octahedral sites, whereas in b) the Co^{2+} cation is located in a centrosymmetric environment that does not permit ordered displacements of the type required to optimize the bonding at Nb. The *c* axis (layer stacking direction) is vertical in both structures.

octahedral Co^{2+}—the slight enhancement of the magnetic moment over the spin-only value results from incomplete quenching of the orbital contribution from the $^4T_{1g}$ state of high-spin Co^{2+} by the trigonal ligand field, and agrees with the value of 4.1 μ_B observed for Co^{2+} in anatase.[12]

For oxides containing metals with variable oxidation states, hopping conduction offers a mechanism for dielectric loss. However, the Co^{2+} oxidation state seems robust in $Ba_8CoNb_6O_{24}$, as indicated both by the magnetic data and the invariance of the cell parameters to processing conditions. The phase can be processed into resonators with a density of 89.6 % of the crystallographic density with a relative permittivity of 31: Q values are sensitive to processing, but resonators with the most dense microstructure (scanning electron micrographic images of sectioned high-Q material shown in Figure S2 and S3 reveal lath- and platelike grains $\geqq 10$ μm thick and of similar aspect to but with larger dimensions than those for $Ba_8ZnTa_6O_{24}$[13]) have Q of 16700 at 3.2 GHz ($Qf = 53200$ GHz). The temperature coefficient of the resonant frequency, τ_f, is 16 ppm K^{-1}. EDS analysis of the grains (Figure S2) at both interior and exterior surfaces of the

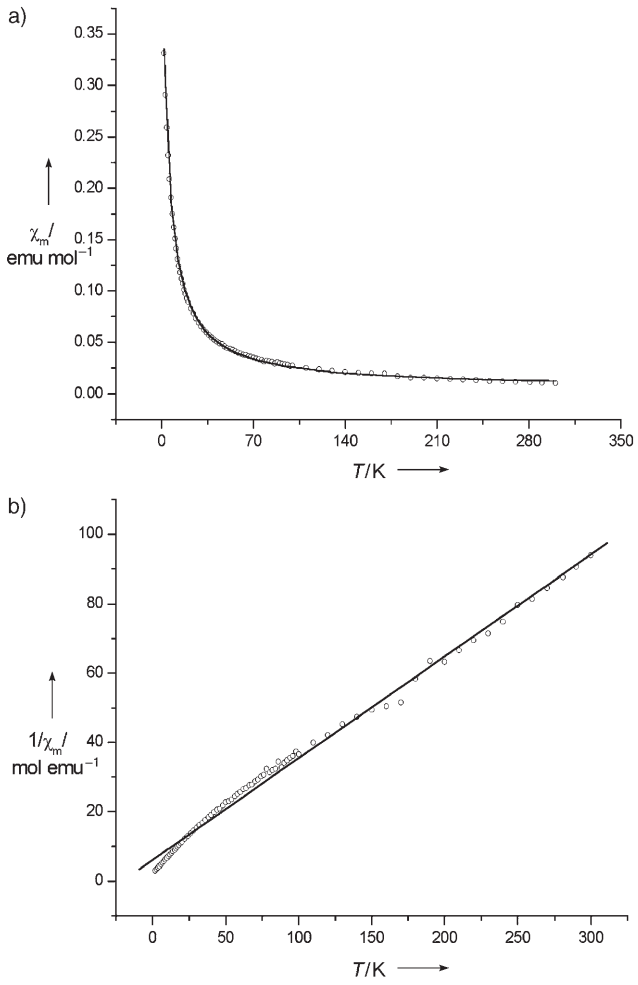

Figure 4. a) Fit of the magnetic susceptibility of $Ba_8CoNb_6O_{24}$ to the Curie–Weiss law. A single-ion Kotani fit gives an unphysical value for the spin-orbit coupling constant and thus the assignment of the observed value of θ to exchange coupling between the cobalt cations is preferred. b) Plot of the inverse susceptibility versus temperature.

resonator ceramics confirms the homogeneity of the Co distribution and the absence of $Ba_3CoNb_2O_9$ perovskite.

The structure of $Ba_8CoNb_6O_{24}$ shows that subtle differences in bonding are sufficient to produce long-range order over nanometer-distance scales even in high-temperature reactions producing complex structures containing solely six coordinate corner-sharing sites. The extension of this motif to compositionally more complex arrays in which three or more metal centers can be manipulated spatially in this manner is now a significant challenge.

Received: January 13, 2005
Revised: August 22, 2005
Published online: November 7, 2005

Keywords: cations · dielectric materials · perovskite phases · transition-metal oxides · X-ray diffraction

[1] B. B. Van Aken, T. T. M. Palstra, A. Filippetti, N. A. Spaldin, *Nat. Mater.* **2004**, *3*, 164.
[2] N. Floros, C. Michel, M. Hervieu, B. Raveau, *J. Solid State Chem.* **2002**, *168*, 11.
[3] T. A. Vanderah, *Science* **2002**, *298*, 1182.
[4] M. T. Anderson, K. B. Greenwood, G. A. Taylor, K. R. Poeppelmeier, *Prog. Solid State Chem.* **1993**, *22*, 197.
[5] G. Trolliard, N. Teneze, P. Boullay, D. Mercurio, *J. Solid State Chem.* **2004**, *177*, 1188.
[6] S. M. Moussa, J. B. Claridge, R. M. Ibberson, M. J. Rosseinsky, S. Clarke, D. Iddles, T. Price, D. C. Sinclair, *Appl. Phys. Lett.* **2003**, *82*, 4537.
[7] B. Mossner, S. Kemmler-Sack, *J. Less-Common Met.* **1986**, *120*, 203.
[8] M. W. Lufaso, *Chem. Mater.* **2004**, *16*, 2148.
[9] Z. Li, J. Sun, L. You, Y. Wang, J. Lin, *J. Alloys Compd.* **2004**, *379*, 117.
[10] T. Siegrist, T. A. Vanderah, *Eur. J. Inorg. Chem.* **2003**, 1483.
[11] M. C. Cadee, D. J. W. Ijdo, *J. Solid State Chem.* **1981**, *40*, 314.
[12] A. Manivannan, G. Glaspell, M. S. Seehra, *J. Appl. Phys.* **2003**, 6994.
[13] P. K. Davies, A. Borisevich, M. Thirumal, *J. Eur. Ceram. Soc.* **2003**, *23*, 2461.
[14] A. Salinas-Sanchez, J. L. Garcia-Munoz, J. Rodriguez-Carvajal, R. Saez-Puche, J. L. Martinez, *J. Solid State Chem.* **1992**, *100*, 201.

